Nuclear Engineering and Technology 53 (2021) 2953–2959

Contents lists available at ScienceDirect

Nuclear Engineering and Technology

journal homepage: www.elsevier.com/locate/net

Original Article

# A practical power law creep modeling of alloy 690 SG tube materials

Bong-Sang Lee*, Jong-Min Kim, June-Yeop Kwon, Kwon-Jae Choi, Min-Chul Kim

*Korea Atomic Energy Research Institute, Yuseong, Daejeon, 34057, South Korea*

ARTICLE INFO

*Article history:*
Received 12 January 2021
Received in revised form
22 February 2021
Accepted 5 March 2021
Available online 11 March 2021

*Keywords:*
Power law creep
Parameter optimization
Alloy 690
Steam generator tube

ABSTRACT

A new practical modeling of the Norton's power law creep is proposed and implemented to analyze the high temperature behaviors of Alloy 690 SG tube material. In the model, both the stress exponent $n$ and the rate constant $B$ are simply treated as the temperature dependent parameters. Based on the two-step optimization procedure, the temperature function of the rate constant $B(T)$ was determined for the data set of each $B$ value after fixing the stress exponent $n$ value by using the prior optimized function at each temperature. This procedure could significantly reduce the numerical errors when using the power law creep equations. Based on the better description of the steady-state creep rates, the experimental rupture times could also be well predicted by using the Monkman-Grant relationship. Furthermore, the difference in tensile strengths at high temperatures could be very well estimated by assuming the imaginary creep stress related to the given strain rate after correcting the temperature effects on the elastic modulus.



## 1. Introduction

Steam generator tube rupture (SGTR) in nuclear power plants has been a concern of environmental contamination in a severe accident scenario. Since the thin walls of steam generator tubes comprise a substantial portion of the reactor pressure boundary, the integrity of SG tubes should be assured in an operating pressurized water reactor (PWR). Traditionally, the focus has been on corrosion related attacks, such as primary water stress corrosion cracking (PWSCC) and outer diameter stress corrosion cracking (ODSCC). As a result, the Alloy 690 material, which is known to be more resistant to stress corrosion cracking (SCC) attacks, has replaced the conventional Alloy 600 material [1,2]. After the Fukushima accident in 2011, the failure probabilities of SG tubes at a high temperature have been the focus of evaluating the risk of SGTR within a severe accident scenario [3,4].

The MELCORE code is often used to analyze the failure probability of SG tubes at high temperatures [5]. The code uses a creep rupture model based on the Larson-Miller parameter (LMP) [6]. The LMP model is simple and has a good capability to extrapolate a long-term creep rupture time from a relatively short laboratory database. However, the LMP model purely correlates the experimental rupture time to the applied test conditions. It may be more appropriate to apply it to a long-term creep damage under a constant stress condition. On the other hand, the creep damage during a severe accident accumulates within only several hours or days [7]. Also, the applied stress and temperature conditions change during the period. In this case, a more comprehensive creep model is necessary to include the effects of deformation history and loading conditions on the rupture time.

The power law models of creep deformation are widely used to correlate the steady-state creep rate with the applied stress at a test temperature. Mechanism based models of the power law equations have been proposed by several researchers [8–14]. The temperature dependence of the power law parameters has been considered as a thermally activated creep process. However, in any case, the real creep behaviors of engineering materials do not generally match with the theoretical models.

In this paper, the power law creep model is treated simply as a phenomenological model. Apart from a sophisticated mechanism, emphasis is given to the optimization procedure of the numeric parameters of the model equations. The proposed two-step optimization procedure of parameter determination could reduce the prediction errors of creep behaviors in different temperatures. The phenomenological model may also be used to estimate the difference in tensile flow stress levels at a high temperature region.

* Corresponding author.
*E-mail address:* bongsl@kaeri.re.kr (B.-S. Lee).

https://doi.org/10.1016/j.net.2021.03.004

As a practical power law approach to predict the creep failure of Alloy 690 SG tube materials, the background of the model, the experimental creep data of the test material, the optimization procedure of the parameters, and the prediction capability of the proposed model are described in this paper.

## 2. Materials and experiments

The test material is a Ni-Cr-Fe alloy, which is designated as Alloy 690 for PWR SG tubes. The dimensions of tubes are 19.05 mm in outer diameter and 1.07 mm in thickness. The chemical composition of the material is as shown in Table 1.

A series of creep rupture tests were conducted in the temperature range of 650–850 °C. An electromechanical testing machine (R&B® Model RB-301) was used for uniaxial creep tests. Steady-state creep rates and rupture times were measured at various combinations of the applied stress and temperature. Test specimens were machined along the longitudinal direction of a tube. The geometry and dimensions of the test specimens are shown in Fig. 1. The strain of the specimens was determined as the extension between the upper and lower loading pins divided by the initial length of the reduced section of the specimen since a high temperature extensometer could not be used for the tube specimens.

Tensile tests were carried out at various temperatures, including the creep test conditions. An electromechanical testing machine (MTS® Model Insight-50) was used for uniaxial tensile tests. The same specimens as illustrated in Fig. 1 were also used for tensile tests. Tensile tests were conducted under a constant extension rate condition while creep tests were conducted under a constant load condition. The strain rate in the tensile tests was $4.6\text{x}10^{-4}$/sec. The tensile properties measured at various test temperatures up to 900 °C are summarized in Table 2.

## 3. Description of the practical power law creep model

At a homologous temperature higher than $0.5T_m$, where $T_m$ is the melting point of the material in Kelvin, the steady-state creep rate is often represented by a power law creep model as below [8]:

$$\dot{\varepsilon}_{ss} = A \cdot \sigma^n \cdot \exp\left[-\frac{Q_C}{RT}\right] \quad (1)$$

where $\dot{\varepsilon}_{ss}$ is the steady-state creep rate, $A$ is the material constant, $\sigma$ is the applied stress, $n$ is the power law stress exponent, $Q_c$ is the activation energy for the creep process, $R$ is the gas constant, and $T$ is the temperature. Equation (1) is often called the Norton's power law. Based on the functional form of equation (1), the experimental data of the steady-state creep rate show a linear relationship with the applied stress in a logarithmic scale at a given temperature.

From a more theoretical point of view, the power law creep model can be written with the form of the so-called Dorn creep equation [9].

**Table 1**
Chemical composition of the Alloy 690 SG tube material.

| Element | C | Mn | Si | S | P | Ni | Cr | Mo |
|---|---|---|---|---|---|---|---|---|
| wt.% | 0.020 | 0.493 | 0.265 | 0.0006 | 0.005 | 59.16 | 29.27 | 0.028 |

| Element | Cu | Co | Al | Ti | Nb | N | B | Fe |
|---|---|---|---|---|---|---|---|---|
| wt.% | 0.012 | <0.010 | 0.165 | 0.245 | <0.010 | 0.020 | <0.0005 | 10.3 |

$$\dot{\varepsilon}_{ss} = A_0\left(\frac{G\Omega}{kT}\right)\left(\frac{D}{b^2}\right)\left(\frac{\sigma}{G}\right)^n \quad (2)$$

where $A_o$ is a dimensionless constant, $D$ is the coefficient of lattice self-diffusion, $G$ is the shear modulus, $\Omega$ is the atomic volume, $b$ is the length of Burgers vector, $k$ is the Boltzman constant, $T$ is the temperature, $\sigma$ is the applied stress, and $n$ is the stress exponent.

When the dislocation glide or climb controls the creep deformation, the power law exponent or the stress exponent would be theoretically 3–5 [10,11]. However, in most engineering metals and alloys, the stress exponents are larger than the theoretical values. This is known as a result of back stress from microstructural variables [12]. Practically, the stress exponent should be treated as a phenomenological value [13,14].

Even though the fundamental creep models like equations (1) and (2) may provide some physical images of the time-dependent creep process, the real creep deformation could not be accurately predicted by the fixed forms. In this paper, a more flexible form of the power law creep model is proposed for the Alloy 690 SG tube material. The main idea is that the two parameters of the proposed model equation (3), i.e., the stress exponent $n$ and the rate constant $B$, are simply treated as the temperature dependent variables, which imply all physical parameters in equations (1) and (2). The parameters are simply determined by a numerical optimization process:

$$\dot{\varepsilon}_{ss} = B \cdot \sigma^n \quad (3)$$

where $B$ and $n$ are defined as the functions of temperature.

This assumption is very plausible since the deformation processes could be slightly changed with temperature, even though the apparent creep mechanism remains the same. The temperature dependent $B(T)$ and $n(T)$ parameters can compensate the effects of the mechanism variation within a temperature range. This idea may have been widely used in the analysis of experimental data sets.

However, a new and most important feature of the current model is a two-step optimization procedure for the rate parameter $B$ by using the results of the once-through determination of parameters $n$. The modified procedure of parameter optimization could reduce the prediction errors significantly and then improve the applicability of the power law creep model to analyze the high temperature deformation and failure. The optimization procedure and the model prediction results are explained in detail in the next section.

## 4. Results and discussion

### 4.1. Creep tests

Fig. 2 shows the creep curves of the test material at various conditions. The material clearly showed a steady-state creep region and tertiary creep region while the primary creep region is almost negligible.

Fig. 3 shows the relations between the steady-state creep rate and the applied stress in a logarithmic scale. At each temperature, the power law relationships are well demonstrated by the straight lines in a logarithmic scale. The slope of each data set, which represents the stress exponent $n$, varies from 3.8–6.6 increasing with a temperature decrease.

Fig. 4 shows the temperature dependency of the stress exponent $n$ values, which increase with decreasing temperature. In this paper, the apparent values of the stress exponents are represented by the following form of the fitting curve:

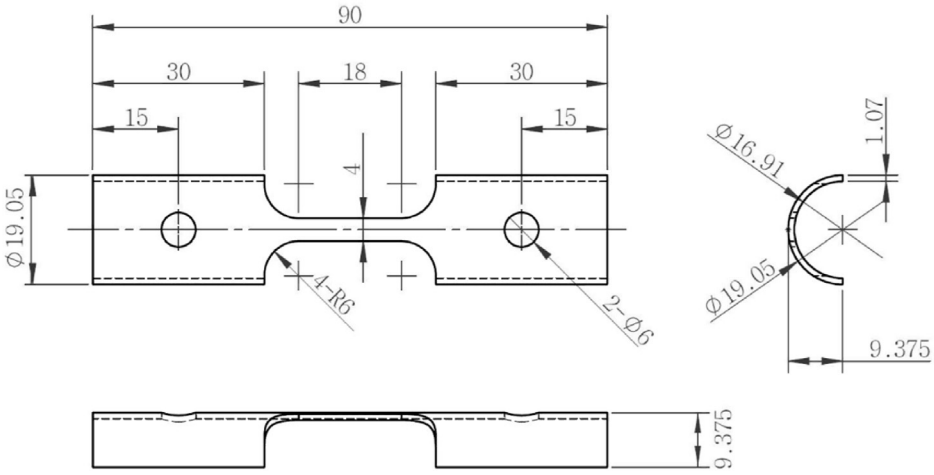


**Fig. 1.** Geometry of creep and tensile test specimens.

**Table 2**
Tensile properties of the Alloy 690 SG tube material.

| Temp (°C) | YS (MPa) | UTS (MPa) | Elongation (%) |
|---|---|---|---|
| 25 | 333 | 743 | 52 |
| 200 | 275 | 644 | 46 |
| 300 | 264 | 627 | 48 |
| 400 | 262 | 620 | 48 |
| 500 | 251 | 593 | 46 |
| 600 | 231 | 536 | 42 |
| 650 | 224 | 465 | 43 |
| 700 | 220 | 408 | 40 |
| 750 | 216 | 294 | 34 |
| 800 | 203 | 224 | 51 |
| 850 | 143 | 153 | 38 |
| 900 | 109 | 123 | 49 |

$$n = 559.9*\exp\left(-\frac{T}{128.1}\right) + 3.0.(\text{units}\cdot\text{in}\cdot\text{MPa}\cdot\text{and}\cdot{}^{\circ}\text{C}) \quad (4)$$

The formula of the fitting curve was arbitrarily selected to represent the data trend while the limit value of 3.0 was fixed to approach a theoretical $n$ value of 3.0 at a high temperature [10].

Fig. 5-(a) shows the temperature dependence of the rate constants $B$ in a logarithmic scale, which were determined by the once-through analysis of the measured data in Fig. 3. It should be noted that the stress exponent $n$ and the proportional coefficient $B$ are not completely independent in the optimization procedure of the given data sets. In the previous paragraphs, the stress exponent $n$ was fitted as a function of temperature by equation (4). Therefore, the temperature dependence of the rate constant $B$ should also be re-analyzed by fixing the stress exponents with the fitted values.

After the two-step optimization process, the estimation of the temperature dependency of the rate constant $B$ showed a better fit, as shown in Fig. 5-(b) compared to Fig. 5-(a). The data points in Fig. 5-(b) are fitted by an exponential formula as below:

$$\log B = -971.5\cdot\exp\left(-\frac{T}{149.6}\right) - 5.109(\text{units}\cdot\text{in}\cdot\text{MPa}\cdot\text{and}\cdot{}^{\circ}\text{C}) \quad (5)$$

By using the fitted equations (4) and (5), the steady-state creep rates can be estimated at an arbitrary combination of the applied stress and temperature.

Fig. 6 compares the measured data of the steady-state creep rates to the ones predicted by the proposed model equations (3)~(5). The standard deviation of the prediction error was only 20%, which is considered good enough in predicting the engineering creep data. Therefore, the power law relations in equations (3)~(5) are appropriate to predict the creep behavior of the test material when the parameters are optimized by the two-step procedure proposed in this paper.

From an engineering point of view, the creep model should also be able to predict the failure time at various conditions. Since the proposed power law model can estimate the steady-state creep rate accurately, it can also be used to predict the creep rupture time.

Conventionally, the Monkman-Grant (MG) relationship has been used to correlate the steady-state creep rate and the rupture time, especially in the power law creep region [15]:

$$\log(t_r) + m\cdot\log\left(\dot{\varepsilon}_{ss}\right) = C_{MG} \quad (6)$$

where $t_r$ is the rupture time, $m$ and $C_{MG}$ are the MG exponent and MG constant of the materials, respectively. This relationship is known to be valid over a large range of loading conditions and materials.

Fig. 7 plots the measured data of the rupture time with the measured values of the steady-state creep rates in a logarithmic scale. The MG relationship of Alloy 690 is fitted by the following equation:

$$\log(t_r) = -0.808\cdot\log\left(\dot{\varepsilon}_{ss}\right) - 0.234 \quad (7)$$

Finally, the creep rupture time of each test condition can be estimated by using equations (3)~(5) and (7). Fig. 8 plots the result of the rupture time prediction in all test conditions, where the prediction is defined as the following:

$$\text{Prediction} = (\text{rupture time predicted}) / (\text{rupture time measured}) \times 100\% \quad (8)$$

The standard deviation of the rupture time prediction is about 30%, which is also small from the view point of creep life analysis.

The rupture time prediction in Fig. 8 showed an approximately linear bias with temperature while there is some scatter. Fig. 8 indicates that the prediction of rupture time may be non-conservative at higher temperature. However, this may not be a general case but rather originates from the statistical nature of MG (Monkman-Grant) relationship. Moreover, the linear bias can be easily compensated by a separate model, such as a modified MG

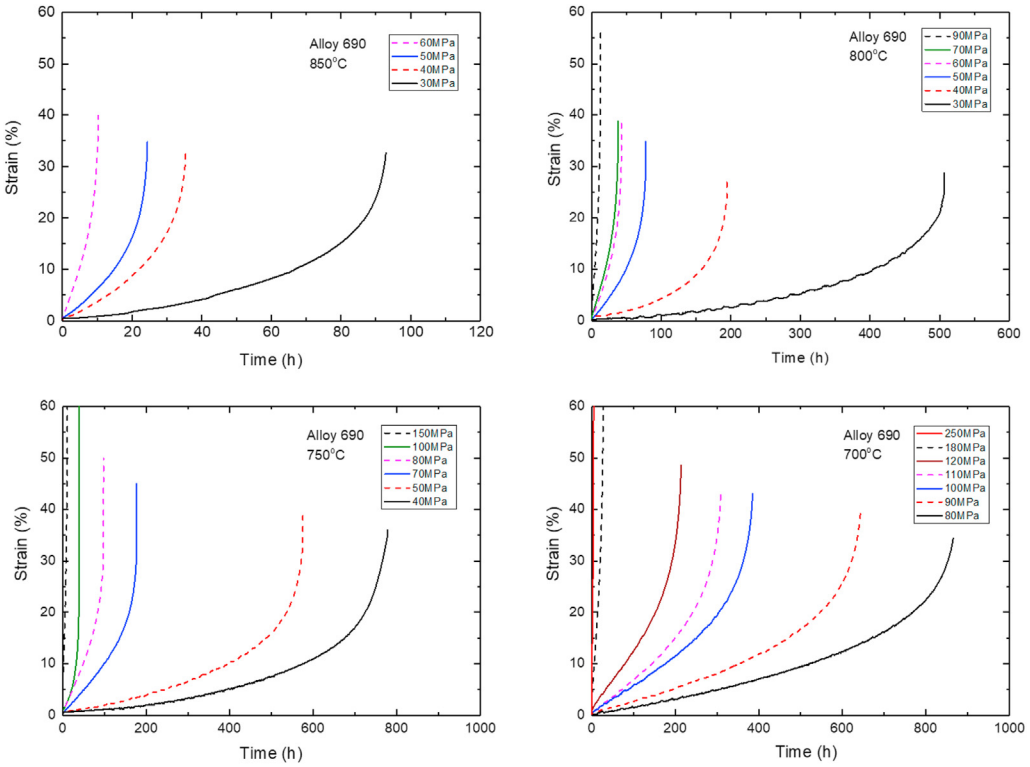


**Fig. 2.** Creep curves of Alloy 690 SG tube material.

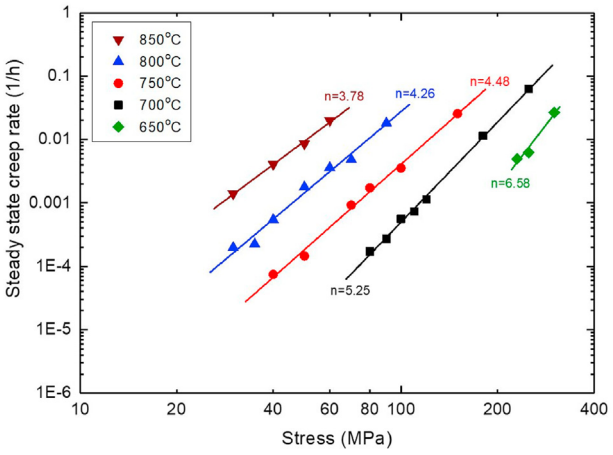


**Fig. 3.** Power law creep analysis of Alloy 690 SG tube material test data.

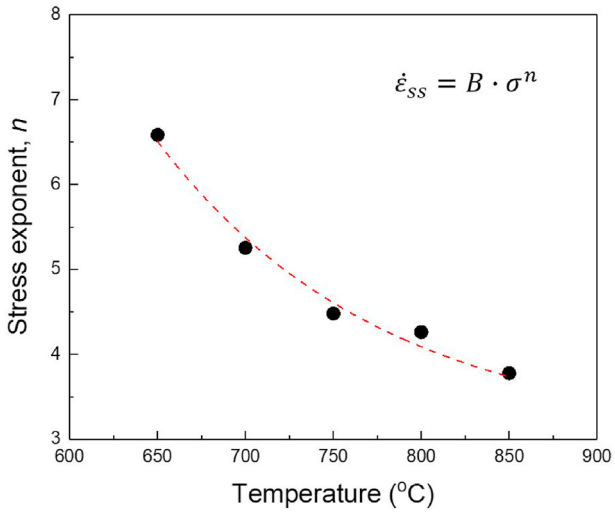


**Fig. 4.** Temperature dependence of the stress exponent, *n*, in power law creep model.

relationship considering the rupture strain [16]. At this moment, the prediction capability of the proposed model is considered sufficiently accurate to evaluate the creep behavior of Alloy 690 material. Further refinement of the proposed model will be made after obtaining a more general trend from larger data sets.

### 4.2. Tensile tests

Besides the creep tests, the tensile test data at high temperature could also imply a certain portion of creep effects. Fig. 9 shows the engineering tensile stress-strain curves at high temperatures under the constant strain rate of $4.6 \times 10^{-4}$/sec. The stress-strain curves at 300–600 °C were slightly shaky. This is a typical phenomenon that is believed to be an effect of dynamic strain aging at this temperature range [17].

From Fig. 9, the tensile curves in 700–900 °C showed a plateau after maximum loads resembling a quasi-steady-state creep behavior. The flow stress is nearly constant at a constant strain rate in a relatively large range of strain like a steady-state creep region. For a very first approximation, we might assume that the difference in the flow stress of tensile curves could result from the creep effects in the temperature range of 700–900 °C, as illustrated in Fig. 10. This assumption may become an initial step to develop more comprehensive constitutive equations at a high temperature deformation. Even though it is not the purpose of the current paper, the preliminary idea was applied to predict the flow stress

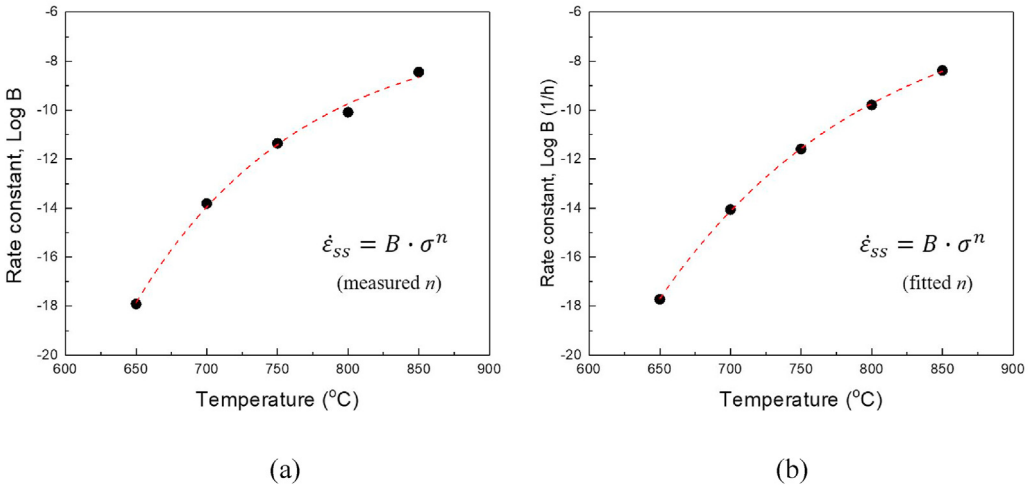


**Fig. 5.** Temperature dependence of the rate constant, $B$. (a) based on the measured $n$ values (b) based on the $n$ values fitted by eq. (4).

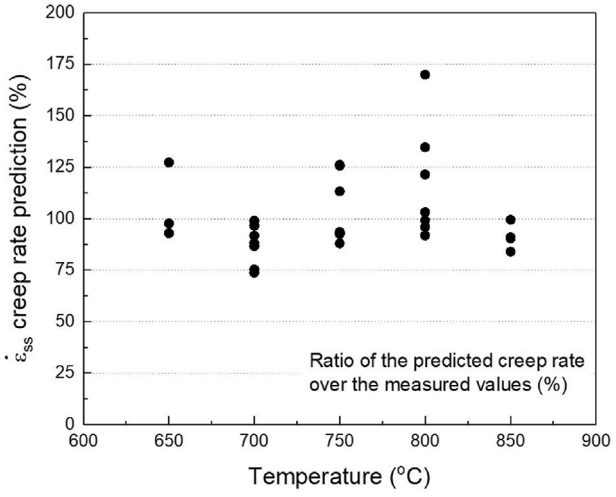


**Fig. 6.** Comparisons of the steady-state creep rates predicted by the proposed model to the measured data at different temperatures.

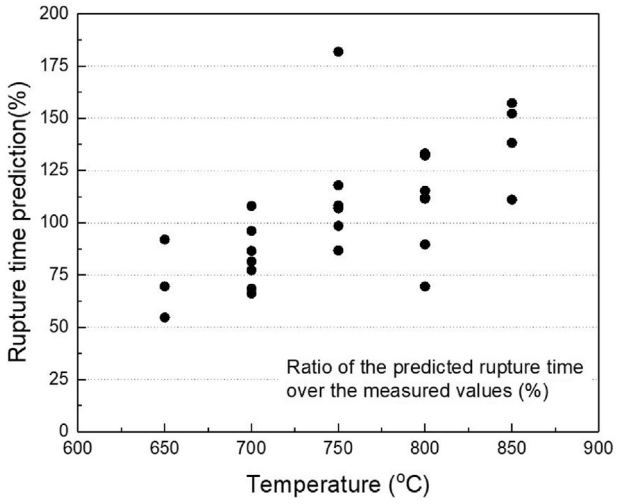


**Fig. 8.** Comparisons of the predicted rupture time to the measured data at different temperatures.

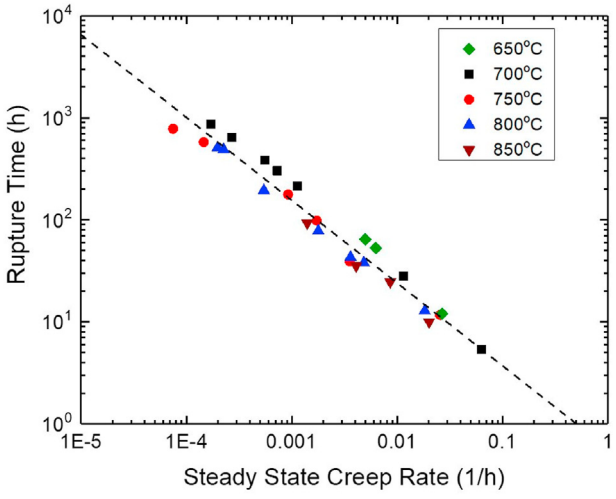


**Fig. 7.** Monkman-Grant relations of Alloy 690 SG tube material.

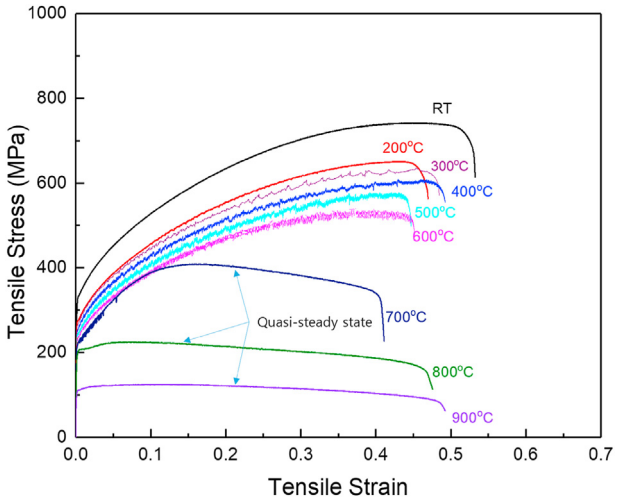


**Fig. 9.** Engineering tensile stress – strain curves of Alloy 690 SG tube material at high temperatures.

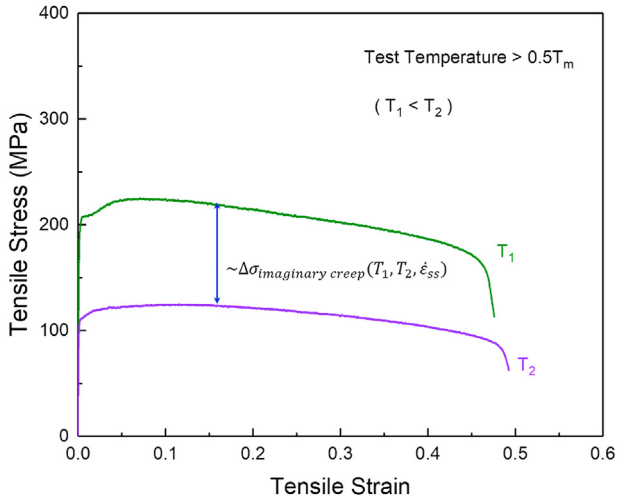


**Fig. 10.** Approximation of the creep effects in tensile curves at high temperatures.

differences at high temperatures for the tensile curves shown in Fig. 9.

Without a comprehensive constitutive model, the difference in flow stress at different temperatures is assumed the same as the difference in the imaginary creep stress to reproduce the tensile strain rate of $4.6\text{x}10^{-4}$/sec, as shown in Fig. 10. For convenience, in this paper, the ultimate tensile strength values were selected as the representative values of the flow stress. The imaginary creep stress is defined as an arbitrary stress at which the calculated steady-state creep rate at a given temperature becomes the same as the tensile strain rate.

Fig. 11-(a) plots the measured tensile strength values with the calculated imaginary creep stresses at 650, 700, 750, 800, 850, and 900 °C. They showed a good linear relationship, but the slope was 0.87, which should be 1.0 to indicate the same stress differences between the tensile and creep behaviors. For clarification, the tensile stress-strain curves were only shown at 100°C intervals in Fig. 9 while the tensile properties at 650, 750, and 850°C are tabulated in Table 2.

Based on equation (2), it can be pointed out that the temperature dependence of the shear modulus may have affected the values of the imaginary creep stress difference. As a result, the authors tried to correct the data of Fig. 11-(a) by considering the temperature effects on the shear modulus of the material. The temperature dependence of the elastic modulus for the Alloy 690 material was acquired from a literature survey [18]. The temperature dependence of the shear modulus was assumed to be the same as the elastic modulus.

In Fig. 11-(b), the calculated imaginary creep stresses were normalized by the ratio of the elastic modulus $E$ as defined below:

$$\text{Ratio of modulus} = E\ (\text{at temperature})/E\ (\text{average in the range}) \quad (9)$$

As shown in Fig. 11-(b), the differences in the tensile flow stresses at a high temperature were very well predicted by using the imaginary creep stress with the proposed power law creep model after the temperature dependence of the elastic modulus was considered. It is notable that the creep test data were actually absent at the highest temperature (900 °C), which was purely estimated from the proposed model equations.

Also, it is notable that the plateau stress in Fig. 10 is not the same as the steady-state creep stress at the given tensile strain rate. The steady-state creep rate is generally achieved under a constant structure condition or a constant back stress [11,14], but the tensile deformation produces a varying structure with the strain [19,20]. This might have made the imaginary creep stress different from the expected steady-state creep stress.

It should be noted that the proposed creep model was based on the experimental data from the longitudinal specimens. Actual creep failure of SG tubes can occur due to circumferential stress caused by internal pressure, and the creep behavior of the SG tube circumferentially would be different from that in the longitudinal direction. Unfortunately, creep test data in the circumferential direction are very scarce due to the complexity in testing. Therefore, the current model is limited to longitudinal data only. However, the methodology will be useful in the same manner in the circumferential direction if a sufficiently credible database is acquired in this direction. Research is ongoing to develop a credible method to test and analyze the mechanical properties in the circumferential direction of tubes [21].

## 5. Conclusions

A practical power law creep model is proposed for the Alloy 690 SG tube material. In the model, both the stress exponent $n$ and the rate constant $B$ are simply treated as the temperature dependent

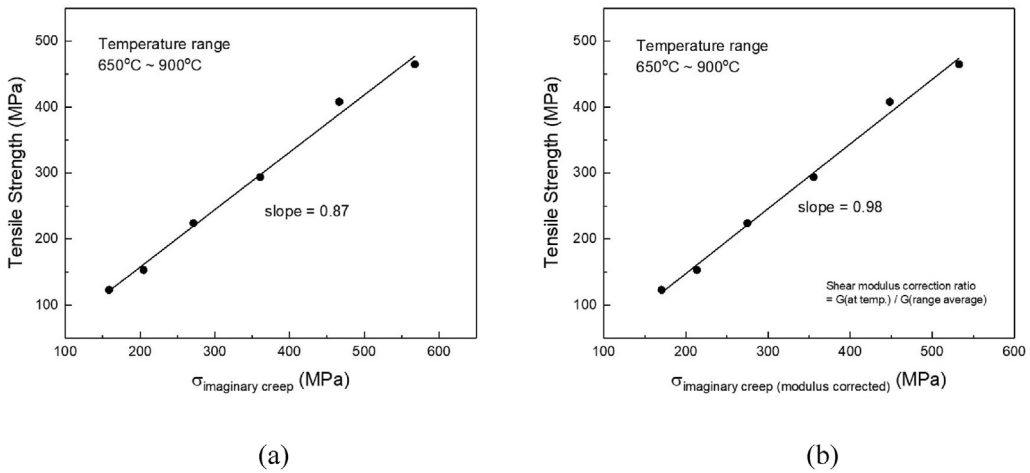


**Fig. 11.** Prediction of the tensile strengths at high temperatures based on the difference in the imaginary creep stresses. (a) without modulus compensation. (b) after modulus compensation at each temperature.

parameters. The most important part of the proposed model is a two-step optimization procedure for the rate parameter *B*. The temperature function of the rate constant *B(T)* should be optimized for the *B* values obtained after fixing the stress exponent with the prior optimized function values at each temperature. This procedure could significantly reduce the prediction errors of the power law creep model.

Based on the better description of the steady-state creep rate, the experimental rupture time could also be well predicted by using the conventional Monkman-Grant (MG) relationship. Furthermore, the difference in tensile strengths at high temperatures could be well predicted by assuming the imaginary creep stress related to the given strain rate after correcting the temperature effects on the elastic modulus.

## Declaration of competing interest

The authors declare that they have no known competing financial interests or personal relationships that could have appeared to influence the work reported in this paper.

## Acknowledgement

This work was supported by the National Research Foundation of Korea (NRF) grant funded by the Korea government (MSIT) (2017M2A8A4015156).

## References

[1] P.E. MacDonald, V.N. Shah, L.W. Ward, P.G. Elliso, Steam Generator Tube Failures, U. S. NRC, NUREG/CR-6365, INEL-95/0383, 1996.
[2] K.J. Karwoski, G.L. Maker, M.G. Yoder, U.S. Operating Experience with Thermally Treated Alloy 690 Steam Generator Tubes, U. S. NRC, 2007. NUREG-1841.
[3] S. Sancaktar, M. Salay, R. Lyengar, A. Azarm, S. Majumdar, Consequential SGTR Analysis for Westinghouse and Combustion Engineering Plants with Thermally Treated Alloy 600 and 690 Steam Generator Tubes, U. S. NRC, 2018. NUREG-2195.
[4] SGTR Severe Accident Working Group, Risk Assessment of Severe Accident-Induced Steam Generator Tube Rupture, U. S. NRC, 1988. NUREG-1570.
[5] Y. Liao, K. Vierow, MELCOR analysis of steam generator tube creep rupture in station black out severe accident, Nucl. Technol. 152 (2005) 302–313.
[6] F.R. Larson, J. Miller, A time-dependence relationship for rupture and creep stresses, Trans. ASME 74 (1952) 765–771.
[7] Y. Liao, S. Guentay, Potential steam generator tube rupture in the presence of severe accident thermal challenge and tube flaws due to foreign object wear, Nucl. Eng. Des. 239 (2009) 1128–1135.
[8] F.H. Norton, The Creep of Steels at High Temperatures, McGraw-Hill, New York, 1929.
[9] A.K. Mukherjee, J.E. Bird, J.E. Dorn, Experimental correlations for high-temperature creep, ASM Trans. Quart. 62 (1969) 155–179.
[10] O.D. Sherby, P.M. Burke, Mechanical behavior of crystalline solids at elevated temperature, Prog. Mater. Sci. 13 (1968) 325–390.
[11] M.E. Kassner, Fundamentals of Creep in Metals and Alloys, Elsevier, Amsterdam, 2009.
[12] B. Derby, M.F. Ashby, Power-laws and A-n correlation in creep, Scripta Metall. 18 (1984) 1079–1084.
[13] A.M. Brown, M.F. Ashby, On the power-law creep equation, Scripta Metall. 14 (1980) 1297–1302.
[14] R.W. Evans, B. Wilshire, Creep of Metals and Alloys, Institute of Metals, London, 1985.
[15] F. C Monkman, N.J. Grant, An empirical relationship between rupture life and minimum creep rate in creep-rupture tests, Proc. Am. Soc. Test. Mater. 56 (1956) 593–620.
[16] W.G. Kim, J.M. Kim, M.C. Kim, Creep deformation and rupture behavior of alloy 690 tube, Trans. KPVP 16 (2020) 49–55. https://doi.org/10.20466/KPVP.2020.16.1.049.
[17] H. Hanninen, M. Ivanchenko, Y. Yagodzinskyy, V. Nevdacha, U. Ehrnsten, P. Aaltonen, Dynamic strain aging of Ni-base alloys INCONEL 600 and 690, in: Proceedings of the 12th International Conference on Environmental Degradation of Materials in Nuclear Power System – Water Reactors, Salt Lake City, USA, August 14-18, 2005.
[18] Special Metals Corporation, INCONEL Alloy 690 Specification, SMC-079, 2009, https://www.specialmetals.com/tech-center/alloys.html.
[19] B.S. Lee, S.W. Nam, J.H. Hong, A phenomenological model for transient creep behaviors based on the steady state creep properties, Scripta Mater. 35 (1996) 379–384.
[20] B.S. Lee, H. Stamm, S.W. Nam, A phenomenological model of creep transient at power law region, in: Oikawa, et al. (Eds.), Strength of Materials, The Japan Institute of Metals, 1994, pp. 595–598.
[21] J.M. Kim, M.C. Kim, Derivation of transverse tensile properties of Alloy 690 steam generator tubes under ring-tensile specimen and finite element analysis (PVP2018-84828), in: Proceedings of ASME 2018 Pressure Vessels & Piping Division Conference (PVP 2018), Prague, Czech Republic, July 15-20, 2018.